

# CDKL5 belongs to the same molecular pathway of MeCP2 and it is responsible for the early-onset seizure variant of Rett syndrome

Francesca Mari<sup>1,†</sup>, Sara Azimonti<sup>3,†</sup>, Ilaria Bertani<sup>3</sup>, Fabrizio Bolognese<sup>3</sup>, Elena Colombo<sup>4</sup>, Rossella Caselli<sup>1</sup>, Elisa Scala<sup>1</sup>, Ilaria Longo<sup>1</sup>, Salvatore Grosso<sup>2</sup>, Chiara Pescucci<sup>1</sup>, Francesca Ariani<sup>1</sup>, Giuseppe Hayek<sup>5</sup>, Paolo Balestri<sup>2</sup>, Anna Bergo<sup>3</sup>, Gianfranco Badaracco<sup>3</sup>, Michele Zappella<sup>5</sup>, Vania Broccoli<sup>4</sup>, Alessandra Renieri<sup>1</sup>, Charlotte Kilstrup-Nielsen<sup>3</sup> and Nicoletta Landsberger<sup>3,\*</sup>

<sup>1</sup>Medical Genetics, <sup>2</sup>Department of Pediatrics, University of Siena, Policlinico 'Le Scotte', 53100 Siena, Italy,

<sup>3</sup>Dipartimento di Biologia Strutturale e Funzionale, Università dell'Insubria, 21052 Busto Arsizio (VA), Italy,

<sup>4</sup>Department of Stem Cell Research, San Raffaele Scientific Institute, 20132 Milano, Italy and <sup>5</sup>Child Neuropsychiatry, Azienda Ospedaliera Senese, 53100 Siena, Italy

Received February 16, 2005; Revised April 14, 2005; Accepted May 16, 2005

**Rett syndrome (RTT) is a severe neurodevelopmental disorder almost exclusively affecting females and characterized by a wide spectrum of clinical manifestations. Most patients affected by classic RTT and a smaller percentage of patients with the milder form 'preserved speech variant' have either point mutations or deletions/duplications in the *MECP2* gene. Recently, mutations in the *CDKL5* gene, coding for a putative kinase, have been found in female patients with a phenotype overlapping with that of RTT. Here, we report two patients with the early seizure variant of RTT, bearing two novel *CDKL5* truncating mutations, strengthening the correlation between *CDKL5* and RTT. Considering the similar phenotypes caused by mutations in *MECP2* and *CDKL5*, it has been suggested that the two genes play a role in common pathogenic processes. We show here that *CDKL5* is a nuclear protein whose expression in the nervous system overlaps with that of *MeCP2*, during neural maturation and synaptogenesis. Importantly, we demonstrate that *MeCP2* and *CDKL5* interact both *in vivo* and *in vitro* and that *CDKL5* is indeed a kinase, which is able to phosphorylate itself and to mediate *MeCP2* phosphorylation, suggesting that they belong to the same molecular pathway. Furthermore, this paper contributes to the clarification of the phenotype associated with *CDKL5* mutations and indicates that *CDKL5* should be analyzed in each patient showing a clinical course similar to RTT but characterized by a lack of an early normal period due to the presence of seizures.**

## INTRODUCTION

Rett Syndrome (RTT, OMIM 312750) is a progressive neurological disorder primarily affecting females with an incidence of approximately 1:15 000 born females (1,2). The disorder is characterized by a wide spectrum of phenotypes. In the classic form, after 6–18 months of almost normal development, patients display a developmental arrest, followed by a regression with loss of speech and purposeful hand use and

appearance of postnatal microcephaly, stereotypic hand movements, ataxia, hand-apraxia and abnormal breathing. At this stage, similarities with autistic behavior are present. Later, there is a limited amelioration followed, in older girls, by a final somatic and neurologic deterioration. Up to 80% of patients experience epileptic episodes (1,3). In addition to classic RTT, some variants have been described presenting some features of the classic form but displaying differences in disease onset and severity.

\*To whom correspondence should be addressed. Tel: +39 0331339406; Fax: +39 0331339459; Email: landsben@uninsubria.it

†The authors wish it to be known that, in their opinion, the first two authors should be regarded as joint First Authors.

A very few cases of familial RTT made it initially difficult to determine the mode of inheritance of this disorder, but the virtual absence of affected males suggested an X-linked dominant inheritance pattern (1). Consistent with this, it was shown that mutations in the methyl-CpG-binding protein 2 gene (*MECP2*) located in Xq28 are the primary cause of RTT (4–6). As a matter of fact, ~80% of patients with classic RTT carry mutations within *MECP2*, whereas only 20–40% of patients affected by RTT variants are mutated within *MECP2* (7–9). Recently, mutations in another X-linked gene, cyclin-dependent kinase-like 5 (*CDKL5*) located in Xp22, have been identified in patients affected by an RTT-like phenotype or the early-onset seizures variant of RTT (Hanefeld variant) (10–12).

MeCP2 is a broadly expressed nuclear protein binding to DNA methylated at CpG dinucleotides through a conserved methylated CpG-binding domain (MBD) (13). Through its ability to recruit chromatin-remodeling complexes containing histone deacetylase activities (HDAC) as well as histone methyltransferase activities, MeCP2 is able to abrogate gene expression by modifying chromatin structure (14,15). Furthermore, by interacting directly with a component of the basal transcriptional machinery, TFIIB, MeCP2 seems to be able to repress transcription in a chromatin independent manner (16). Eventually, this methyl-binding protein is able to compact a nucleosomal array on its own (17), suggesting that altogether MeCP2 exerts a number of effects on chromatin structure and gene expression.

Mice null for *Mecp2*, both male hemizygotes and female homozygotes, manifest phenotypes resembling that of RTT (18,19). Importantly, the conditional deletion of *Mecp2* in postmitotic neurons recapitulates these features, demonstrating that neuronal dysfunction is the cause of the deficiencies in these mice (19). Furthermore, the rescue of the RTT-like phenotype in *Mecp2* knock-out mice by expression of *Mecp2* only in postmitotic neurons underscores the importance of this protein for proper brain function (20). In accordance with this, *Mecp2* expression is particularly high in neurons and its timing of expression correlates with neuronal maturation (21). Initially, mutations in the *MECP2* gene were proposed to cause RTT because of a defect in preventing unscheduled transcription throughout the genome (22), but only minor changes in gene expression are observed in microarray studies using mRNAs from *Mecp2* mutant mice as well as RTT patients (23,24). The recent demonstration that *Hairy2A* in *Xenopus* and *Bdnf* (brain-derived neurotrophic factor) are direct MeCP2 target genes suggests that only specific loci may be deregulated in RTT (25–27). It is important to note that an ~2-fold derepression of *Bdnf* was observed in *Mecp2*-deficient cells (26) indicating that only subtle changes in gene expression may be present in RTT patients. Importantly, Chen *et al.* (26) demonstrated that *Bdnf* repression is regulated by MeCP2 phosphorylation; in particular, upon membrane depolarization of cultured neurons, MeCP2 becomes phosphorylated and specifically detach, together with the Sin3A/HDAC complex, from the *Bdnf* promoter, thus permitting transcriptional activation. However, the upstream events regulating the observed phenomena and the involved kinase(s) remain unknown.

CDKL5 is a hitherto rather uncharacterized protein containing a conserved serine/threonine kinase domain in its N-terminal, sharing homology to members of the mitogen-activated protein (MAP) kinase and cyclin-dependent kinase (CDK) families (28). However, the kinase activity of CKDL5 has never been demonstrated. The recent discovery that *CDKL5* mutations can cause a phenotype overlapping RTT might indicate that the two proteins belong to the same genetic pathway (10).

In this paper, we report the identification of additional *CDKL5*-mutated patients, reinforcing the link between the gene and RTT. Given the apparent importance of MeCP2 phosphorylation and the evident involvement of CDKL5 in RTT, we found it challenging to deeply investigate the CDKL5 protein concerning its developmental expression pattern, protein interaction and functional activity.

Here, we demonstrate that *Cdkl5* expression in developing mice significantly overlaps with that of *Mecp2*. The possibility that these two proteins belong to the same molecular pathway is reinforced by their capability to interact *in vitro* and *in vivo*. Importantly, the interaction surface on the methyl-binding protein is given by a region including the last residues of the transcriptional repression domain (TRD) and the C-terminal portion of the protein. Interestingly, this region includes residues frequently mutated in RTT patients; moreover, a missense mutation associated with an atypical variant of RTT has been reported (see the MeCP2 mutation frequency at the URL: <http://mecp2.chw.edu.au/>). Eventually, we demonstrate that CDKL5, according to its primary structure, harbors a kinase activity, which mediates MeCP2 phosphorylation *in vitro*, further reinforcing the idea that they are associated in the same molecular pathway.

## RESULTS

### Identification of two novel *CDKL5* mutations leading to the early seizure RTT variant

We observed two female patients, aged 7 and 2, who show many characteristics of RTT. Both patients have a normal head circumference and lack the characteristic first normal period due to the presence of seizures. A detailed clinical description is reported subsequently.

*Patient 1.* This patient is the first child, presently aged 7. The mother has a second child, a male, who is normal. The mother had a normal pregnancy and delivery. From the first days of life, her parents noticed the occurrence of flexion spasms involving the entire body, lasting a few seconds and followed by relaxation. An electroencephalogram (EEG) conducted at 1 month was reported as normal, but a subsequent EEG at 3 months showed the presence of paroxysmal spike-wave activities, more evident in the left temporal region, and biparietal sharp waves, made more active by sleep. A brain magnetic resonance imaging (MRI) showed the presence of an arachnoid cyst in the left temporal region. An anti-epileptic treatment was subsequently instituted but epileptic fits remained in time. She was able to sit alone at 18 months and she has never been able to walk alone. She has never uttered a word and she was always unable to use her hands to take objects. Hand-mouthing and clapping activities are present since the

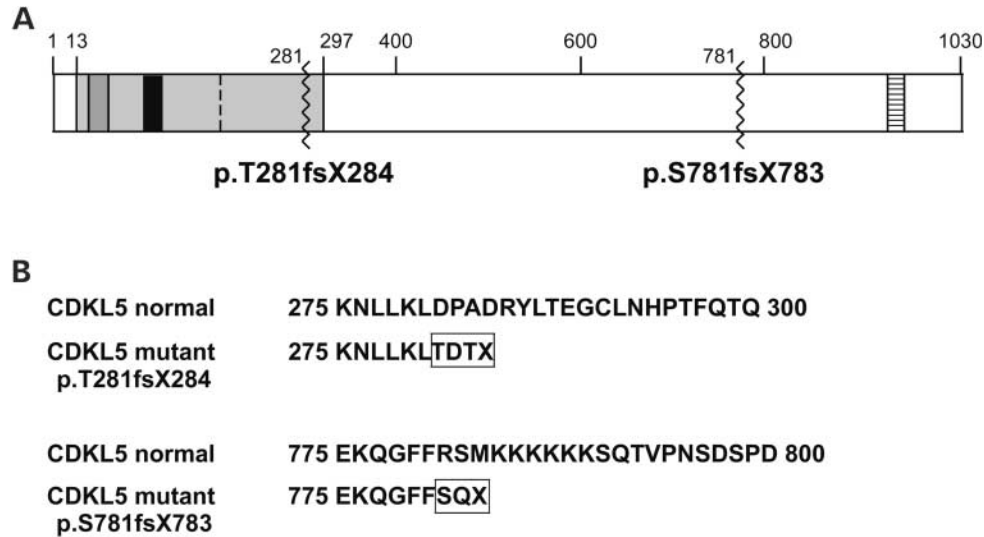


**Figure 1.** Schematic representation of the CDKL5 protein with mutation position and alignment between the normal and the mutated amino acid sequences. (A) The predicted human CDKL5 protein and the positions of the new identified mutations are represented. The catalytic domain (light gray box) contains an ATP binding site (dark gray box) and the serine–threonine protein kinase active site (black box). The conserved Thr–Xaa–Tyr phosphorylation sites are indicated with a sketch line. The signal peptidase I Serine active site, located in the C-terminal region of the protein, is represented by the striped box. The positions of the two frame-shift deletions (p.T281fsX284 and p.S781fsX783) are indicated by zigzag lines. Numbers at the top refer to the amino acid positions. (B) Alignment between the normal and the mutated CDKL5 sequences. In patient 1, the deletion led to protein truncation in position 284, after a short stretch of incorrect amino acids (boxed). The deletion creates a protein lacking the final portion of the kinase domain. In patient 2, the frame-shift deletion creates a stop codon in position 783, after a short stretch of abnormal amino acids (boxed). The deletion falls in the C-terminal portion of the protein outside the predicted catalytic domain.

second year of life. Her head circumference is presently 51.3 cm (25–50°). She is able to interact at a preverbal level. Generalized convulsions characterized by tonic–clonic jerks, eyes revulsion and chewing movements of the mouth are now present once a week in spite of various treatments including valproate and benzodiazepin. She has gastroesophageal reflux and she is treated accordingly. In addition, she has stypsis, cold extremities and bruxism.

**Patient 2.** This patient is a female, now aged 2. The mother had a normal pregnancy and delivery. Birth weight, length and head circumference were in the normal range. Parents referred a sudden awakening at 3 months of age. They also referred that at 5 months of age, she had some episodes, in which she suddenly opened her eyes remaining a few moments with staring eyes, during her sleep. The psychomotor development was normal in the first 6 months, when the first episodes diagnosed as seizures were noted. The seizures resembled infantile spasms, although the EEG did not show hypsarrhythmia. They were difficult to control with various anti-epileptic drugs and they persisted during the following months. In the first months of age, she had gastroesophageal reflux. She was able to utter some words at 12 months and to walk alone at 20 months. A brain MRI performed at 10 months, ophthalmologic examination, biochemical analyses and screening for metabolic disorders were normal. She presently shows autistic features according to DMSIV. She is able to hold an object in her hands. She has hand-mouthing and clapping stereotypic activities. Her head circumference is still in the normal range (48.5 cm, 50°cent). She can occasionally utter one word. Partial convulsions, characterized by a sudden opening of the arms, are still present, in spite of

various treatments. The EEG shows paroxistic activities in the frontal region. In addition, constipation is referred, whereas scoliosis, kyphosis and cold extremities are not present.

Considering the phenotype of the two patients, we decided to analyze both *MECP2* and *CDKL5*. In particular, we excluded the presence of *MECP2* point mutations (including exon 1) and gross rearrangements by DHPLC and qPCR, respectively. DHPLC analysis of *CDKL5* revealed the presence of two different ‘*de novo*’ frame-shift mutations (Fig. 1A). Case 1 showed a 10 bp deletion in exon 11 (c.838\_847del10, p.T281fsX284) leading to the loss of almost 800 amino acids of the protein, after a short stretch of incorrect amino acids (Fig. 1B). In case 2, we identified a 1 bp deletion in exon 16 (c.2343delG, p.S781fsX783) leading to protein truncation in position 783 (Fig. 1B).

#### **MeCP2 and CDKL5 do not interact at transcriptional level**

Even though, by whole-mount *in situ* hybridization performed on brain of *Mecp2*-deficient mice, it has been demonstrated that *Cdkl5* expression is independent of *MeCP2* expression (12), we tested whether the two genes interact at a transcriptional level in humans by real-time qPCR. For this purpose, we analyzed both *CDKL5* and *MECP2* mRNA levels in lymphoblastoid cell lines from patients with *MECP2* early truncating mutations and *CDKL5* mutations, respectively. The expression levels were quantified by the ddCt method. Figure 2 shows the columns corresponding to the mean values of the ddCt ratios obtained for control and mutated samples in both *MECP2* and *CDKL5* assays. The statistical analysis of the expression levels of both the genes indicated that there is

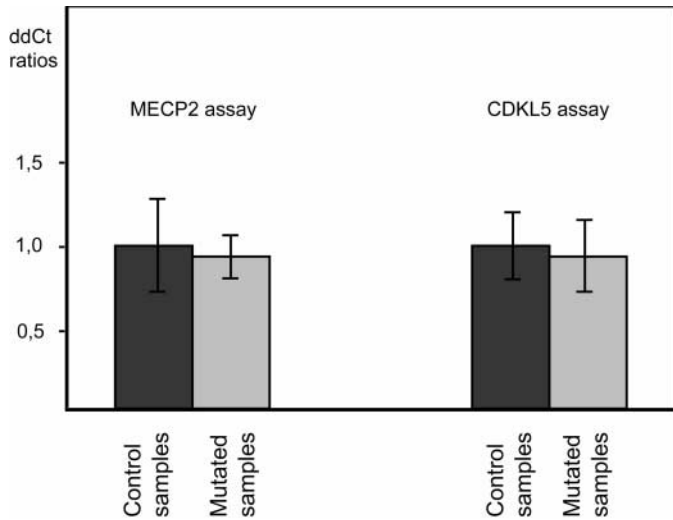


**Figure 2.** Real-time qPCR analysis. On the left, *MECP2* assay. Mean values of *MECP2* ddCt ratios and standard deviations (SD) of five control samples (dark gray column) and three *MECP2* mutated samples (light gray column). On the right, *CDKL5* assay. Mean values of *CDKL5* ddCt ratios and SD of five control samples (dark gray column) and three *CDKL5* mutated samples (light gray column).

not a significant difference between control and mutated samples ( $P > 0.05$ ). In conclusion, these data, together with the results obtained in mouse brain (12), suggest that there is not an epistatic relationship between *CDKL5* and *MeCP2*.

### ***Mecp2* and *Cdkl5* expression patterns are significantly overlapping in embryonic and postnatal mouse brains**

As already published, *Mecp2* has a widespread expression throughout the mature brain specifically confined to differentiated neurons (29). However, some heterogeneity in *Mecp2* expression levels has been observed in early postnatal stages where neurons that were generated early and are more mature have a stronger expression (21). Hence, *Mecp2* expression gradually broadens and gets enhanced in the brain during early postnatal stages. We investigated *Cdkl5* expression during neuronal maturation and compared it with that of *Mecp2*. As for *Mecp2*, *Cdkl5* expression is weakly detectable at late stages of embryogenesis while strongly enhanced from P1 onwards (compare Fig. 3A with E and Fig. 3B with F). *Cdkl5* expression is first observed in neural cells that have reached their final position in the cortical plate (Fig. 3B and data not shown). In the early postnatal days, a high enhancement of *Cdkl5* expression is observed, reaching a stable peak at P10 (Fig. 3F and H). At this stage, the regions with the highest *Cdkl5* expression are the neocortex (Cx), the piriform cortex (pc), the hippocampus (hip), the amygdala complex (ac) and the dorsal geniculate nucleus (dgc) as similarly found for *Mecp2* (Fig. 3E and F). At this stage, in particular, the majority of the cortical neurons are highly expressing both *Cdkl5* and *Mecp2* (Fig. 3G and H). Interestingly, the observed general increase of *Cdkl5* expression in the first postnatal stages may be closely correlated with neural maturation and synaptogenesis as already proposed for *Mecp2* (21,29). On the same line, the

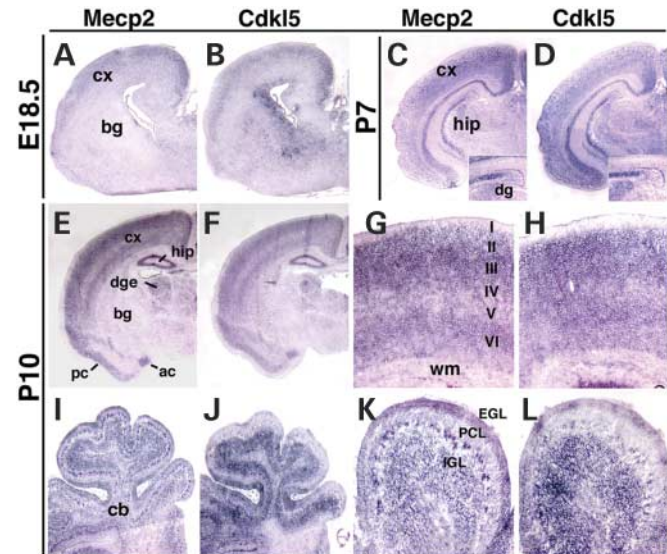


**Figure 3.** *Mecp2* and *Cdkl5* expression patterns during neural differentiation. *Mecp2* (A) and *Cdkl5* (B) expressions are first detected in E18.5 brains in the neurons migrated into the cerebral cortex (cx). (C and D) Sections of posterior forebrain hybridized for *Mecp2* and *Cdkl5*, respectively. Note the strong expression in the hippocampus (hip) of both genes. Inserts in (C) and (D) show gene expression in the dentate gyrus (dg). (E–H) *Mecp2* and *Cdkl5* expressions in medial forebrain sections (E and F) and in cerebral cortex (G and H) of mouse at P10. Expression of both genes is enriched in all the six layers of the cortex, piriform cortex (pc), amygdala complex (ac), hippocampus (hip) and dorsal geniculate thalamic nucleus (dgc). (I–L) Mouse P10 cerebellum labeled for *Mecp2* and *Cdkl5* expressions. Note that although both genes are expressed in external granular layer (EGL), Purkinje cellular layer (PCL) and internal granular layer (IGL), their expression level in any specific layer is differently modulated (compare *Mecp2* and *Cdkl5* staining in PCL in K and L). bg, basal ganglia; wm, white matter.

delay in the increase of *Cdkl5* expression in the dentate gyrus (dg) with respect to the hippocampal area may follow the different phases of neurogenetic maturation of these two fields (inserts in Fig. 3C and D). However, not all the brain regions show a comparable levels of *Cdkl5* and *Mecp2* expression. For instance, at P10 in the cerebellum, the two genes show different levels of expression in specific cerebellar domains. In fact, a strong *Mecp2* but weak *Cdkl5* staining is detected in the Purkinje neurons; whereas high *Cdkl5* and low *Mecp2* expression levels were found in granular cells (Fig. 3I–L). This indicates that different *Cdkl5* and *Mecp2* expression levels may coexist in the same cells suggesting independent mechanisms of gene regulation in such tissues.

### ***MeCP2* and *CDKL5* are directly interacting *in vitro* and *in vivo***

To understand whether *MeCP2* and *CDKL5* belong to the same molecular pathway, we went ahead analyzing the possibility that the two proteins may even be directly interacting. We addressed this point performing a classical glutathione *S*-transferase (GST) pull-down assay in which a GST–*MeCP2* fusion protein, expressed in *Escherichia coli*, was immobilized on a Glutathione–Sepharose resin and challenged with h*CDKL5* translated *in vitro*. As shown in Figure 4A, *CDKL5* is retained on the GST–*MeCP2* resin (lane 4), whereas no *CDKL5* is

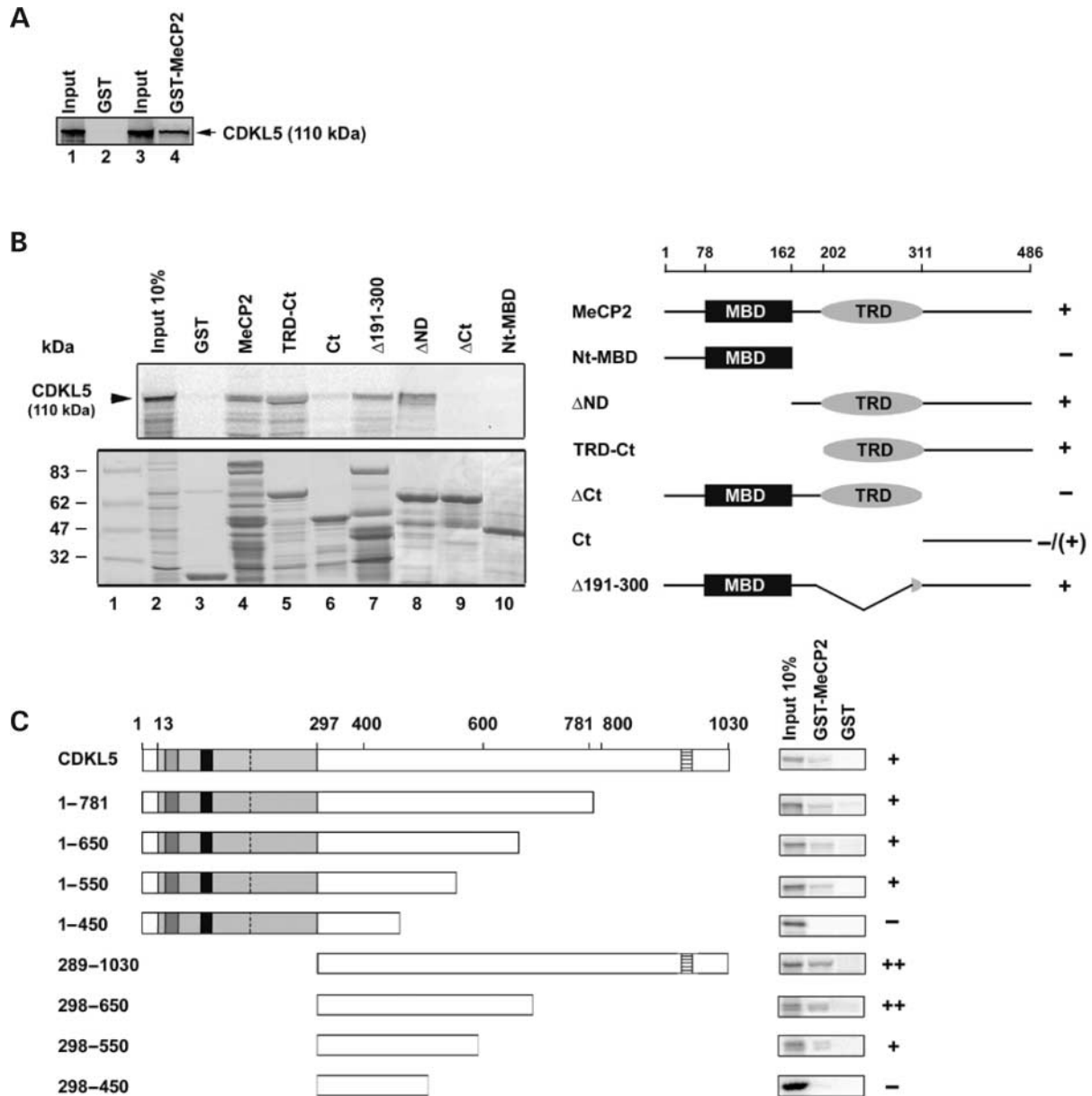


**Figure 4.** CDKL5 and MeCP2 interact *in vitro*. (A) GST pull-down assay in which *in vitro* translated [ $^{35}$ S]methionine labeled CDKL5 was incubated with immobilized recombinant GST and GST-MeCP2. Retained proteins were separated on an 8% SDS-PAGE and CDKL5, indicated to the right, were visualized by autoradiography. 'Input' (lanes 1 and 3) corresponds to 10% of *in vitro* translated CDKL5 used in the binding reactions (lanes 2 and 4). (B) *In vitro* translated full-length  $^{35}$ S-labeled hCDKL5 was incubated with immobilized recombinant GST and the GST-MeCP2 derivatives schematically illustrated on the right. Retained CDKL5 is visualized in the autoradiogram shown in the upper panel, whereas resin coupled GST and GST-MeCP2 derivatives were detected by Coomassie staining (lower panel). The obtained results are schematized on the right indicating with + and - the presence and absence, respectively, of interaction. (C) Full-length CDKL5 and different truncated derivatives were translated *in vitro* and incubated with resins containing GST or GST-MeCP2. The panels in the right part illustrate the amount of CDKL5 retained on the resins and the strength of the interaction is indicated with + and -. By Coomassie staining, it was verified that comparable amounts of GST and GST-MeCP2 were present in the pellets (data not shown).

seen on the GST resin (lane 2). Approximately 5% of CDKL5 used in the binding reaction was found to bind GST-MeCP2 as estimated by comparing the retained protein (lane 4) with the 10% loaded in 'Input' (lane 3). To understand which regions of MeCP2 are engaged in the identified interaction, the pull-down assay, described in Figure 4A, was repeated using deletion derivatives of the methyl-binding protein (Fig. 4B). First, MeCP2 was divided into N- (1-162) and

C-terminal (163-486) portions. The N-terminal part contains the well-known MBD (13), whereas the linker region, the TRD and the last residues of the protein, including a new structural domain (amino acids 359-430) common with regulatory factors belonging to the forkhead gene family (30), are contained in the C-terminal portion.

The figure indicates that the N-terminal region is unable to associate with CDKL5; accordingly, the C-terminal portion

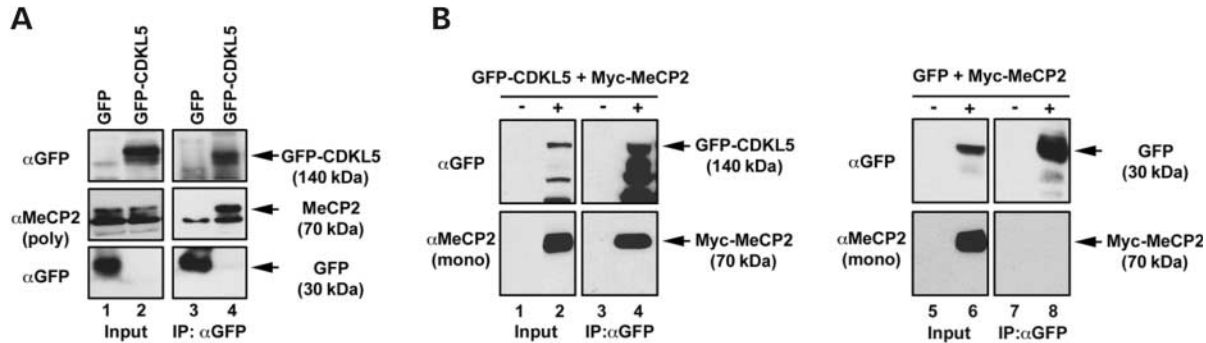


**Figure 5.** CDKL5 and MeCP2 interact also *in vivo*. (A) Coimmunoprecipitation of overexpressed GFP-CDKL5 and endogenous MeCP2. The left panels show a western blot on 10% of the GFP (lane 1) and GFP-CDKL5 (lane 2) human 293T cell extracts used for the immunoprecipitation. To the right, the figure shows GFP (lane 3) and GFP-CDKL5 (lane 4) immunoprecipitated with monoclonal anti-GFP antibody (GFP). Immunoblotting was performed using GFP and anti-MeCP2 polyclonal antibodies (MeCP2). (B) Immunoprecipitation performed with the GFP antibody on overexpressed GFP-CDKL5 and Myc-MeCP2 (left panel). As control, the immunoprecipitation was also performed on cells cotransfected with GFP and MeCP2 (right panel). The input corresponding to 10% of the cell extracts is shown in lanes 1, 2 and 5, 6. Immunoblotting was performed using GFP and anti-MeCP2 monoclonal antibodies.

shows an interaction comparable with the full-length protein. The experiment performed with an MeCP2 derivative containing only the TRD and the C-terminal (202–486) demonstrates that this peptide is perfectly able to pull down CDKL5, therefore excluding the linker region as the main interacting surface. Moreover, the  $\Delta$ Ct derivative containing amino acids 1–311 was significantly impaired in its association with the putative kinase, indicating that the TRD is not sufficient for the association. Eventually, as the isolated C-terminal portion (312–486) is unable to interact with the putative kinase, we reasoned that the main interaction surface might include the residues connecting the TRD with the C-terminal portion. Accordingly, an MeCP2 derivative missing most of the TRD domain, excluding the last 11 amino acids, demonstrates its capability to interact with the kinase.

To identify the interaction surface on CDKL5, we *in vitro* translated the deletion mutants schematically illustrated in Figure 4C and used them in classical GST pull-down assays. By progressively deleting the C-terminal of the kinase, we could show that the region containing amino acids 450–550 is required for the interaction with the methyl-binding protein. However, by comparing the autoradiographic signals, we assume that residues included in the 551–650 region reinforce the association. Furthermore, the catalytic domain is not involved in the interaction because a CDKL5 derivative missing the N-terminal 298 amino acids (298–1030) is still able to associate with MeCP2. Actually, this region seems to negatively influence the CDKL5–MeCP2 interaction, because we reproducibly observed a stronger interaction when the kinase domain was missing.

To summarize, we conclude that MeCP2 and CDKL5 are directly interacting *in vitro* and that a portion of MeCP2, containing the last residues of the TRD and the C-terminal region, is the main surface responsible for this association. Regarding the CDKL5 region interacting with MeCP2, so far we have not been able to reveal neither any significant homology to other factors nor the presence of an already known structural motif.

In order to reveal whether the two proteins physically associate also *in vivo*, coimmunoprecipitation experiments were performed (Fig. 5). We transiently transfected human

293T cells with green fluorescent protein (GFP)–CDKL5, or as a control with GFP, and precipitated the overexpressed proteins from the cell extracts with anti-GFP antibodies (Fig. 5A). A subsequent immunoblotting with polyclonal anti-MeCP2 antibodies revealed that endogenous MeCP2 coprecipitates with overexpressed GFP-CDKL5 (lane 4) but not when GFP alone is overexpressed (lane 3). The capability of the two proteins to interact *in vivo* has also been confirmed by coimmunoprecipitation experiments performed on transfected cells overexpressing both GFP-CDKL5 and Myc-MeCP2 (Fig. 5B). The absence of the MeCP2 signal in untransfected cells (lanes 1, 3 and 5) is due to the fact that in this case, we chose to follow the methyl-binding protein with a commercial monoclonal antibody that increased the specificity of the signal, although reducing its sensibility; it is worthwhile to note that 293T cells have been chosen due to their high efficiency of transfection, even though they are low in abundance of MeCP2.

In conclusion, we have been able to demonstrate that CDKL5 and MeCP2 interact also *in vivo*, a result that is coherent with the fact that transfected GFP-CDKL5 is localized, as MeCP2, in the nucleus (data not shown).

### CDKL5 is a kinase mediating MeCP2 phosphorylation

Given the direct interaction between MeCP2 and CDKL5 and the fact that the two proteins are coexpressed in different brain regions, it was important to understand the functional role of this interaction. CDKL5 is a putative kinase due to the presence of a conserved kinase domain within the protein, but its catalytic activity has never been proven. To reveal a catalytic activity, we exploited the fact that many kinases are able to autophosphorylate and we incubated *in vitro* translated  $^{35}$ S-labeled CDKL5 in the presence of  $[\gamma\text{-}^{32}\text{P}]\text{ATP}$ . In order to discriminate between  $^{35}\text{S}$ - and  $^{32}\text{P}$ -signals, the dried SDS-PAGE was exposed to a series of X-ray films of which the one closest to the gel receives the  $^{35}\text{S}$ - and  $^{32}\text{P}$ -signals, whereas the one farthest away picks up only the signal from  $^{32}\text{P}$ . As seen in Figure 6A, the signal derived from incorporated  $^{35}\text{S}$  does not reach the most distant X-ray-film

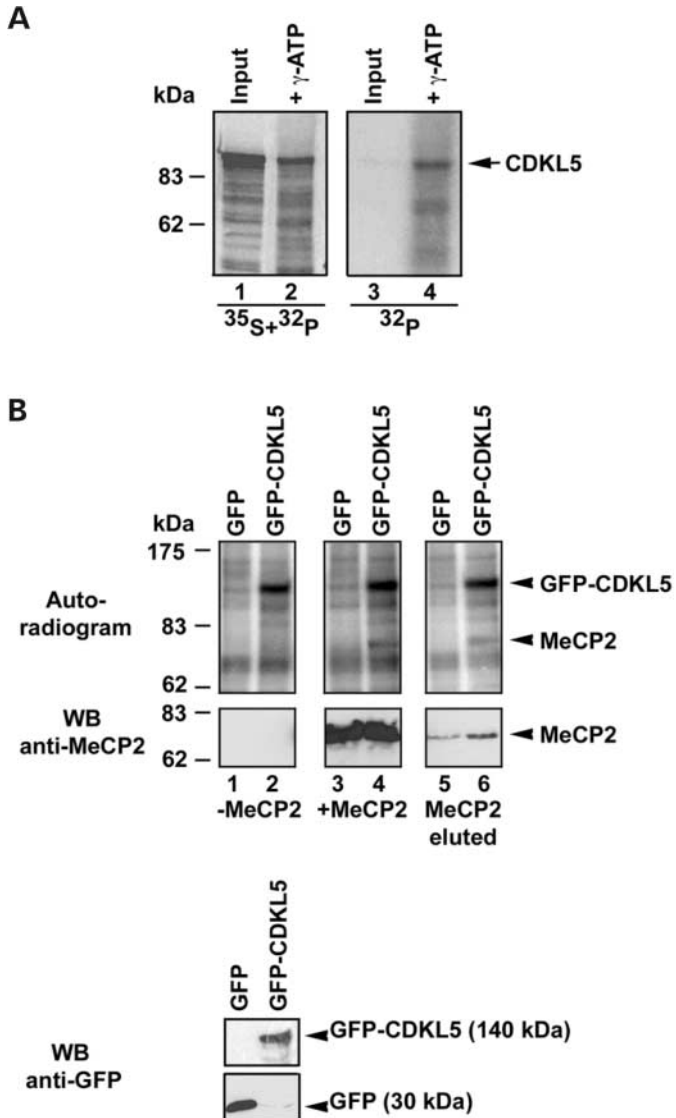


**Figure 6.** CDKL5 possesses a kinase activity and mediates MeCP2 phosphorylation. (A) Autophosphorylation assay in which CDKL5 translated *in vitro*, in the presence of [ $^{35}\text{S}$ ]methionine, was incubated with [ $\gamma$ - $^{32}\text{P}$ ]ATP for 30 min at 30°C. Proteins were fractionated on an 8% SDS-PAGE, the gel dried and exposed to a stack of three X-ray films, so that radioactivity with different  $\beta$ -emission potentials would impress different layers of the films stack. The left panel shows the X-ray film in the stack in contact with the dried gel picking up radioactivity from both  $^{35}\text{S}$  and  $^{32}\text{P}$ , whereas the right panel shows the autoradiogram of the third X-ray film (further from the dried gel), which picks up only the  $\beta$ -emission from  $^{32}\text{P}$ . 'Input' shows *in vitro* translated  $^{35}\text{S}$ -labeled CDKL5 (lanes 1 and 3) whereas '+  $\gamma$ -ATP' shows CDKL5 incubated with  $^{32}\text{P}$  (lanes 2 and 4). The  $^{32}\text{P}$  band in lane 4 indicates that CDKL5 can autophosphorylate (indicated with an arrow). (B) *In vitro* kinase assay in which GFP-CDKL5 or GFP was purified from overexpressing cells and incubated with immobilized Myc-MeCP2 (lanes 3 and 4), immunopurified FLAG-MeCP2 (lanes 5 and 6) or without exogenously added MeCP2 (lanes 1 and 2) in the presence of [ $\gamma$ - $^{32}\text{P}$ ]ATP. After 30 min of incubation, the reaction was loaded on SDS-PAGE and the phosphorylated proteins were revealed by autoradiography (autoradiogram panels). Bands corresponding to phosphorylated GFP-CDKL5 and MeCP2 are indicated to the right. The amount of exogenously added MeCP2 present in each lane was evaluated by western blot using a monoclonal antibody anti-MeCP2 (WB anti-MeCP2 panels). The WB anti-GFP panels represent an aliquot of the immunocomplexes identical in amount to those used for the kinase assay (for details see Materials and Methods).

(lane 3), whereas the addition of [ $\gamma$ - $^{32}\text{P}$ ]ATP leads to a signal corresponding to CDKL5, which is able to penetrate the stack of X-ray films (lane 4), demonstrating that indeed CDKL5 has kinase activity directed against itself.

We next wanted to analyze whether the interaction of MeCP2 with CDKL5 results in the phosphorylation of the methyl-binding protein. To this end, we overexpressed GFP-CDKL5 in mammalian cells, immobilized it on a resin and incubated it with immunopurified-MeCP2 in the presence of [ $\gamma$ - $^{32}\text{P}$ ]ATP. Labeled proteins were separated by SDS-PAGE and visualized by autoradiography. As can be seen in Figure 6B, the incubation of immobilized Myc-MeCP2 with the resin containing the kinase results in its phosphorylation (lane 4). The control performed with purified GFP alone did not cause any phosphorylation of MeCP2 (lane 3). To confirm the result, an identical assay was performed using an immunopurified FLAG-MeCP2. Once again, only in the presence of CDKL5, the methyl-binding protein gets modified (lanes 5 and 6). Moreover, by comparing the amounts of MeCP2 present in each lane (see the western blot in the lower panels), it appears that phosphorylation of the eluted MeCP2 is significantly more efficient (compare lanes 4 and 6). A parallel experiment was performed without the addition of MeCP2 (lanes 1 and 2) to show the specificity of the reaction. The autophosphorylation of GFP-CDKL5 is also confirmed in this experiment, as visualized in lanes 2, 4 and 6. Eventually, to further analyze the specificity of the reaction, we transfected and purified from mammalian cells an unrelated kinase, the CRK kinase (31), and assayed its capability to mediate MeCP2 phosphorylation. The obtained results indicated that in our experimental conditions, this kinase maintains a strong autophosphorylation activity but is unable to cause MeCP2 labeling (data not shown).

## DISCUSSION

RTT is one of the leading causes of mental retardation and developmental regression in females. RTT patients, after an apparently normal development during the first months of life, show characteristic clinical features including microcephaly, hand wringing, autism, seizures and loss of speech. Besides the classical form, several RTT variants have also been described. The phenotypic spectrum of RTT varies from the most severe cases, including the congenital form and the early onset seizure variant (Hanefeld variant), to the milder forms, comprising the 'forme fruste', the preserved speech variant (PSV) and the late regression variant (32).

Mutations in the *MECP2*, located in Xq28, have been identified in almost 80% of classical RTT cases (4-6). On the contrary, only 20-40% of patients affected by RTT variants, mostly PSV, bear mutations in *MECP2* (7-9). The existence of RTT patients without *MECP2* mutations suggests that additional genetic factors might determine this disorder. According to these data, mutations in another X-linked gene, *CDKL5* located in Xp22, have been recently identified in patients with a phenotype overlapping with that of RTT (10-12). These cases showed a strikingly similar clinical course: they had seizures in the first months of life and subsequently developed recognizable RTT features. In particular,

the phenotype of the two patients described by Scala *et al.* (10) meets the criteria for the diagnosis of the RTT early-onset seizure variant.

In the present work, we report the identification of two additional patients with mutations in *CDKL5*. These girls came to our attention for the presence of epileptic seizures. Later on, they developed characteristics typical of RTT such as stereotypic hand movements and hand apraxia. These features were more evident in the older patient (patient 1), in whom a clinical diagnosis of early-onset seizure variant of RTT was promptly suspected. In the younger patient (patient 2), the phenotype was less characteristic and clinical features were intermediate between the early-onset seizure variant of RTT and autism. Considering the phenotype of these two girls, we expected to find *CDKL5* mutations and we indeed identified two different 'de novo' frame-shift mutations. The identification of these two novel mutations reinforces the link between the *CDKL5* gene and the pathogenesis of RTT and suggests that *CDKL5* mutation screening should be performed in patients with the early-onset seizure variant.

*CDKL5* is a hitherto rather uncharacterized protein originally identified as a serine/threonine kinase gene from sequence similarity searches. Sequence comparisons have indicated that *CDKL5* shares homology with members of the MAP kinase family and with cyclin-dependent protein kinases (28). However, its kinase activity has never been demonstrated. *CDKL5* mutations reported so far vary from substitutions in the putative N-terminal catalytic domain to frame-shift mutations in the N- or in the C-terminal portion of the protein (10–12). Whereas it is easy to hypothesize that mutations hitting the kinase domain might influence the catalytic activity of the protein, late truncating mutations could have several effects, such as influencing its stability, cellular localization, protein/protein interactions and/or response to upstream signaling events. Future work will reveal the molecular effects of the identified mutations; however, it is important to note that transfected *CDKL5* seems quite unstable, perhaps indicating that its metabolism is specifically regulated.

Given that *MECP2* and *CDKL5* mutations cause a similar phenotype, it was challenging to investigate whether they belong to the same molecular pathway. We compared the expression patterns of *Mecp2* and *Cdkl5* in embryonic and postnatal mouse brains and we demonstrated that the expression of both proteins increases as neuronal maturation progresses after neurons have reached their final positions inside the cortical plate. Importantly, the two genes generally show a spatial and temporal overlapping expression that is simultaneously activated according to the morphogenetic program specific to each neural district. The obtained results are in favor of a possible involvement of the two proteins in the same developmental pathway. Regarding the cerebellum, *Mecp2* and *Cdkl5* have common areas of expression, although with different expression levels. This may indicate that in some circumstances, the two genes are regulated independently and/or have specific transduction machineries.

We then investigated whether the two proteins interact at the transcriptional level in human lymphoblastoid cell lines, and we excluded this possibility by performing expression studies by real-time qPCR. These results are in accordance

with a previous publication showing that in mouse brain, the absence of *MeCP2* does not modify *Cdkl5* expression (12).

We then decided to analyze whether the two proteins directly interact. By classical pull-down assays, we have been able to demonstrate that *MeCP2* associates with *CDKL5* *in vitro*. The same result has been confirmed *in vivo* by means of coimmunoprecipitation experiments. Importantly, a region of *MeCP2* including the last residues of the TRD and residues belonging to the C-terminal domain represents the main interacting surface. It is worthwhile to note that an analysis of the *MeCP2* mutation database (<http://mecp2.chw.edu.au/>) reveals that residues 301, 302, 305 and 306, belonging to the most C-terminal part of the TRD, are frequently mutated in RTT. Furthermore, the C-terminal contains a hot-spot for Rett mutations and some of them occur in the amino acids close to the TRD, as the 311, 314, 318, 322, 328 and 330. In the future, it will be also important to analyze if any of the RTT mutations affecting this protein domain has lost its capability to interact with *CDKL5*.

Because *CDKL5* is considered a kinase on the basis of sequence homologies, we proceeded analyzing its catalytic activity. To this aim, we performed an autophosphorylation assay and we showed that *CDKL5* is able to phosphorylate itself. This result appeared to be of significant relevance, because it has recently been suggested that *MeCP2* is not only involved in long-term gene silencing, but also in the regulation of dynamic promoters, modulated by extracellular signals (25–27). In particular, in mammals, phosphorylation of *MeCP2* is required for the selective release of the methyl-binding protein from the *Bdnf* promoter, and for its subsequent transcriptional activation (26,27). These findings highlight the importance of *MeCP2* phosphorylation in regulating its activity and indicate the relevance of the disclosure of signaling pathways converging on *MeCP2*. For this reason, we decided to test whether *CDKL5* may exert a kinase activity on *MeCP2*. Our results have shown indeed that an immunopurified *CDKL5* mediates the phosphorylation of an exogenously added *MeCP2*, unraveling a possible function of the interaction. However, further studies are necessary to firmly establish whether *MeCP2* is the main target of *CDKL5* *in vivo*, and whether the biological significance of the interaction between the two proteins is limited to phosphorylation.

To conclude, we have demonstrated that *CDKL5* is the first known kinase capable of mediating *MeCP2* modification *in vitro*: its expression pattern, together with its kinase activity, offers a molecular explanation to its involvement in RTT. However, as it is always the case, the same results pave the ways to more studies. In fact, in the future, it will be interesting to understand which RTT mutations in *MeCP2* abolish the capability of the methyl-binding protein to interact with its kinase and which one modifies residues that are specifically targeted by the enzyme. Moreover, it will be important to characterize the molecular effects of the *CDKL5* mutations associated with RTT as well as the signaling pathways converging on this enzyme.

From a clinical point of view, the features of the two girls reported in this paper and those described in our previous work stress the idea that *CDKL5* mutations are responsible for a specific phenotype, largely overlapping the phenotype previously described as early-onset seizure variant of RTT (10).



Usually in the classic RTT phenotype, seizures and epileptic signs appear in the 80% of cases and only in the third pseudo-stationary stage which starts at 3–10 years of age; on the contrary, in this variant, these symptoms appear early and blur the characteristic onset symptomatology of RTT. Therefore, it will be interesting to clarify why mutations in *CDKL5* generate a phenotype in which seizures develop earlier than in patients with *MECP2* mutations.

It is important to note that other authors have described slightly different phenotypes associated with *CDKL5* point mutations (11,12,33,34). Because these patients are seen by different clinicians, part of this variability may be due to different clinical sensitivity. Moreover, *CDKL5* may cause both the early-onset seizure variant of RTT and a less defined phenotype ranging from autism and mental retardation.

In conclusion, our results contribute to the clarification of the phenotype associated with *CDKL5* and trace out a molecular link between *MeCP2* and *CDKL5*. In addition, this paper indicates that the *CDKL5* gene should be tested in each patient showing a clinical course similar to RTT but lacking of an early normal period due to the presence of seizures.

## MATERIALS AND METHODS

### Patients

We investigated two patients aged 2 and 7 with early development of convulsions, who later developed many characteristics of RTT.

### Molecular analysis of the identified patients

Blood samples were obtained after informed consent. DNA was extracted from peripheral blood using a QIAamp DNA Blood Kit (Qiagen). DNA samples were screened for mutations in the four exons coding for *MECP2* using Transgenic WAVE denaturing high performance liquid chromatography (DHPLC). The analysis of the *MECP2* gene for deletions/duplications was performed as previously described (35). DNA samples were screened for mutations in *CDKL5* by DHPLC. The *CDKL5* coding portion was entirely analyzed using primers and conditions as previously indicated (10). PCR products resulting in abnormal DHPLC profiles were sequenced on both strands using PCR primers with fluorescent dye terminators on an ABI PRISM 310 genetic analyzer (PE Applied Biosystems, Foster City, CA, USA).

### Analysis of *CDKL5* and *MECP2* mRNA levels

RNA was isolated from EBV-transformed lymphoblasts of probands and control individuals following the TRIZOL procedure (Life Technologies). cDNA was synthesized in a 100  $\mu$ l reaction containing total RNA (1–2  $\mu$ g), specific primers (1  $\mu$ M each), dNTP (500  $\mu$ M), RNase inhibitor (0.4 U/ $\mu$ l), 1 $\times$  TaqMan RT buffer, magnesium chloride (5.5 mM), Random Examer (2.5  $\mu$ M) and Multi Scribe Reverse Transcriptase kit (1.25 U/ $\mu$ l) (Applied Biosystems). The reaction was incubated at 25°C for 10 min, 48°C for 30 min and finally at 95°C for 5 min.

Real-time qPCR assays were performed with the fluorescent TaqMan method and an ABI Prism 7700 Sequence Detection System. Primers and probes for *CDKL5* gene were designed using the Primer Express software (Applied Biosystems), following the criteria indicated in the program:

EX9-*CDKL5*-F: CTGAGCAGATGAAGCTTTTCTACAGT  
EX10-*CDKL5*-R: TGAGGATGGTTAACAGCTGGAA  
PROBE: 6-FAM-TCCTCGCTTCCATGGGCTCCG-TAMRA

The *CDKL5* probe contained a fluorophore 5'-FAM as reporter and a 3'-TAMRA as quencher. The GAPDH kit, used as an internal reference, was provided by Applied Biosystems. The GAPDH probe contained a fluorophore 5'-VIC as reporter. We performed separate and multiplex preruns varying the concentrations of primers and probe in order to obtain the highest intensity and specificity of reporter fluorescent signal. PCR was carried out using an ABI prism 7000 (Applied Biosystems) in a 96-well optical plate with a final reaction volume of 50  $\mu$ l. All reactions were prepared from a single PCR Master Mix consisting of: 2 $\times$  TaqMan Universal PCR Master Mix, 300 nM *CDKL5* forward primer, 300 nM *CDKL5* reverse primer, 200 nM *CDKL5* probe, 20 $\times$  GAPDH and HPLC pure water. A total of 100 ng of RNA was dispensed in each of the four sample wells for quadruplicate reactions. Thermal cycling conditions included a prerun of 2 min at 50°C and 10 min at 95°C. Cycle conditions were 45 cycles at 95°C for 15 s and 60°C for 1 min according to the TaqMan Universal PCR Protocol (ABI).

*CDKL5* gene is present in two different isoforms: *CDKL5* isoform II which is transcribed at a very low level in human fetal brain and testis but not in lymphoblastoid cells and *CDKL5* isoform I which is expressed in a wide range of cells including lymphoblastoid cells. We specifically tested the isoform I in lymphoblastoid cell lines of patients.

In order to analyze *MECP2* expression, a commercial assay was purchased from Applied Biosystems (assay code Hs 00172845\_m1, the supplied probe and primers were designed across exons 2 and 3). All reactions were prepared from a single PCR Master Mix consisting of: 2 $\times$  TaqMan Universal PCR Master Mix, 2 $\times$  *MECP2* kit, 2 $\times$  GAPDH and HPLC pure water. A total of 100 ng of RNA was dispensed in each of the four sample wells for quadruplicate reactions. Thermal cycling conditions included a prerun of 2 min at 50°C and 10 min at 95°C. Cycle conditions were 40 cycles at 95°C for 15 s and 60°C for 1 min according to the TaqMan Universal PCR Protocol (ABI). The TaqMan Universal PCR Master Mix and Microamp reaction tubes were supplied by Applied Biosystems.

*MeCP2* is present in two different isoforms: the transcript *MeCP2A* (or *MeCP2 $\beta$* ) comprising four exons, with translation start site in exon 2 and the transcript *MeCP2B* (or *MeCP2 $\alpha$* ) lacking exon 2, with translation start site in exon 1. We have tested only the isoform *MeCP2A* (or *MECP2 $\beta$* ) in lymphoblastoid cell lines of patients, because we used a probe and primers designed across exons 2 and 3.

For these assays, we selected three classic RTT patients with early truncating *MECP2* mutations (two with p.R255X and one with p.R270X) and three *CDKL5*-mutated patients, two previously reported by Scala *et al.* (10) (one with p.R55fsX74 and the other with p.E879fsX908), and one,

described here (with p.S781fsX783) (6). Five known control samples were tested in each assay. All samples were run in quadruplicate. A comparative Ct method, as previously described by Livak (36) (ABI Prism 7700 Sequence Detection System, PE Applied Biosystems) was used to calculate the expression levels of the two genes. Using this calculation, a ddCt ratio of about 1 was arbitrarily assigned to one of the control samples. The non-parametric test of Mann–Whitney with a significance level of 95% was used for the comparison between control and mutated samples.

### Plasmid construction

The cDNA encoding hCDKL5 was obtained from RZPD, Germany (IRATp970G1233D). The entire cDNA was PCR amplified and cloned into pSP65 (Promega) in frame with a C-terminal Myc-tag. The presence of an SP6 promoter in this vector allowed the coupled *in vitro* transcription/translation reactions. pGFP–CDKL5 was cloned by inserting the entire CDKL5 cDNA into *Bgl*II and *Eco*RI sites in pEGFP-C1 (Clontech). pGST–hMeCP2 and pGST–Nt-MBD, containing the cDNAs encoding the entire coding sequence (486 amino acids) or the N-terminal 162 amino acids of the hMeCP2A, respectively, were cloned by insertion of PCR amplified cDNAs into the *Bam*HI site of pGEX-4T-1. pGST-Ct was obtained by PCR cloning the whole C-terminal domain (residues 311–486) into the *Bam*HI site of pGEX-4T-1; pGST-TRD-Ct was produced inserting a PCR fragment coding for the human residues 201–486 into the *Eco*RI/*Sal*I sites of pGEX-4T1. pGST-ΔND and pGST-ΔC1 have been described elsewhere (37). pSG5-FLAG-MeCP2 was cloned by inserting a *Bam*HI-digested PCR fragment, amplified from the human cDNA, in frame with an N-terminal FLAG tag in pSG5 (Stratagene). All constructs based on PCR were verified by PCR. The pCDNA3 vectors encoding for the CRK kinase and the human Myc-MeCP2 were a kind gift of Dr Ferdinando Di Cunto and Dr Berge Minassian, respectively. The GST–MeCP2 derivative missing amino acids 199–300 (pGST–MeCP2Δ199–300) was generously given by Dr Ian Marc Bonapace.

### GST pull-down assays

To map the interacting domain on the methyl binding protein, GST and GST–MeCP2, or its derivatives, were purified from DH5α using Glutathione–Sepharose 4B (Amersham Pharmacia Biotech) according to the manufacturer's instructions. Immobilized GST proteins (~2 μM) were incubated with 10 μl of *in vitro* translated <sup>35</sup>S-labeled CDKL5 for 2 h at 4°C in PBS; 1 mM PMSF. Five washes were performed with PBS; 0.1% Triton X-100; 0.1% NP-40 and retained proteins resolved by SDS–PAGE and detected by autoradiography of the dried gel. GST fusion proteins were visualized afterwards by staining the rehydrated gel with Coomassie blue. *In vitro* translated CDKL5 was obtained using the TNT SP6 Coupled Reticulocyte Lysate System (Promega) with hCDKL5 as template.

The surface of CDKL5 involved in the association with MeCP2 was investigated incubating immobilized GST and GST–MeCP2 with 15–20 μl of *in vitro* translated

<sup>35</sup>S-labeled CDKL5 derivatives, produced using the TNT T7 Quick for PCR DNA (Promega) using hCDKL5 as template. Incubation conditions, washes and analysis of the interacting proteins and the GST fusion proteins utilized were as described earlier.

### *In situ* hybridization

*In situ* hybridizations on frozen sections were performed as previously described (38), with the following modifications. Slides were fixed for 30 min at room temperature in 4% paraformaldehyde in PBS and treated for 5 min with 1 μg/ml Proteinase K in 1 mM EDTA and 20 mM Tris–HCl (pH 7.0). Before hybridization, the slides were washed twice in 2× SSC for 15 min, and incubated in 0.1 M Tris, 0.1 M glycine for at least 30 min. Hybridization solution (60 μl/slide) contained 50% formamide, 5× SSC (pH adjusted with citric acid to 6.0), 5% dextran sulfate, 2 mg/ml heparin, 100 μg/ml tRNA and a 1:100 or 1:50 dilution of the riboprobes. Hybridization occurred overnight at 65°C under coverslips. Following hybridization, slides were washed for 1–2 h in 0.5× SSC, 20% formamide at 65°C. Sections were treated with 10 μg/ml RNase A for 30 min at 37°C in NTE, then washed for 4 h in 0.5× SSC, 20% formamide at 65°C and for 30 min in 2× SSC and blocked for 1 h at room temperature in 1% blocking reagent (ROCHE) in MABT. A 1:5000 dilution of anti-digoxigenin-AP conjugate (ROCHE) was preincubated for at least 1 h in 1% blocking reagent in MABT at 4°C. Slides were incubated with the antibody overnight at 4°C, washed for 6 h in TBST, for 30 min in NTMT and stained using centrifuged BM purple AP substrate (ROCHE) in 0.3% Tween-20 for 12–36 h at 4°C and/or room temperature. Slides were washed in NTMT, then in distilled water and embedded in Aqua PolyMount (Polysciences, USA). Cdkl5 and Mecp2 probes were obtained by *in vitro* transcribing the two full-length murine cDNAs containing untranslated regions.

### Coimmunoprecipitation experiments

For coimmunoprecipitation, HEK 293T cells were plated on 150 mm Petri dishes (Corning) and transiently transfected with pGFP–CDKL5 or pEGFP-C1 with calcium phosphate method. At 36 h after transfection, total cell extracts were prepared with lysis buffer (Tris–HCl 50 mM pH 8.0, NaCl 150 mM, 1% NP-40, 1 mM dithiothreitol, PMSF and a mix of protease inhibitors from SIGMA). Equal amounts of protein were incubated for 1 h with 10 μl of anti-GFP monoclonal antibody (Roche); 50 μl of Protein G-agarose beads (Amersham) were then added and the immunoprecipitate was further incubated for 4 h at 4°C. Immunocomplexes were collected by centrifugation, washed five times with lysis buffer, separated on a 8% SDS–PAGE and blotted to nitrocellulose membrane (Amersham). Filters were blocked in PBS-0.2% Tween plus 5% dried milk and incubated with anti-hMeCP2 rabbit polyclonal antibody or anti-GFP monoclonal antibody. The MeCP2 antibody was a rabbit polyclonal derived from bacterially expressed full-length human cDNA encoding MeCP2 (Fabrizio Bolognese, unpublished data).

### In vitro phosphorylation assays

CDKL5 autophosphorylation was revealed incubating 10  $\mu$ l of *in vitro* translated CDKL5 in 30  $\mu$ l of kinase buffer (20 mM HEPES pH7.4, 10 mM MgCl<sub>2</sub>, 0.5 mM DTT, 200  $\mu$ M sodium orthovanadate) in the presence of 50  $\mu$ M ATP; 5  $\mu$ Ci [ $\gamma$ -<sup>32</sup>P]ATP for 30 min. at 30°C and separated by SDS-PAGE. The dried gel was exposed to a stack of three X-ray films of which the first receives the mixed <sup>35</sup>S- and <sup>32</sup>P-signals, whereas the last picks up only the <sup>32</sup>P signal.

To detect MeCP2 phosphorylation, total cell extracts were prepared and immunoprecipitated with anti-GFP monoclonal antibody as previously described. The immunocomplexes were divided into four aliquots. One was used to control the quality of the precipitation by western blot using the anti-GFP monoclonal antibody. The remaining aliquots were used for the phosphorylation assay. Immobilized Myc-MeCP2 was obtained transfecting pcDNA3-Myc-Mecp2 into HEK 293T cells. After transfection, total cell extracts were prepared with the following lysis buffer: 20 mM HEPES pH 7.4, 150 mM NaCl, 3 mM EDTA, 0.5% NP-40, 1 mM DTT, PMSF and a mix of protease inhibitors (SIGMA). Myc-MeCP2 was immobilized using the anti-C-Myc agarose conjugate (SIGMA) following the manual's instructions. Eluted FLAG-MeCP2 was obtained transfecting pSG5-FLAG-MeCP2 into HEK 293T cells; total cell extracts were prepared as described earlier. FLAG-MeCP2 was immunopurified using E2 view Red ANTI-FLAG M2-agarose (SIGMA) and eluted with the specific tripeptide from SIGMA. Immobilized Myc-MeCP2 or the eluted FLAG-MeCP2 was added to the GFP-immunocomplexes equilibrated in kinase buffer. An aliquot corresponding to 10% was used in a western blot assay performed with the monoclonal anti-MeCP2 antibody. About 7  $\mu$ Ci of [ $\gamma$ -<sup>32</sup>P]ATP and 25  $\mu$ M of unlabeled ATP were added to the remaining sample and the reaction incubated for 30 min at 30°C. The reaction was stopped by the addition of Laemmli buffer and directly loaded onto an 8% SDS-PAGE; <sup>32</sup>P-labeled protein was detected by autoradiography.

### ACKNOWLEDGEMENTS

We sincerely thank the members of the families for participation in this study. We are indebted to Dr Mitsuhiro Suzuki for the generous gift of the GST fusion hMeCP2 derivatives, to Dr Ferdinando Di Cunto for the CRK kinase, to Dr Ian Marc Bonapace for the  $\Delta$ 191–300 GST-MeCP2 derivative, to Dr Berge Minassian for the human Myc-MeCP2 and to Dr Gabriele Cevenini for the statistical analysis. We are grateful to all the members of the laboratories for stimulating discussion, and we thank the anonymous referees for important suggestions. This research was partially funded by Telethon (N.L.), International Rett Syndrome association (N.L.), Rett Syndrome Foundation (C.K.-N.), Cofinanziamento MURST-Università dell'Insubria (G.B.) and FIRB 2001 (Fondo per gli Investimenti della Ricerca di Base) from Ministero dell'Istruzione, dell'Università e della Ricerca (N.L.). This work was also supported by Telethon grants GGP02372A and GTF02006, by the Emma and Ernesto Rulfo Foundation, by MIUR (FIRB 01) and by the University of Siena (PAR 2001, PAR 2002 and PAR 2004) to A.R.

and by Telethon grants GGP04141 and FIRB RBNE015242 to V.B.

*Conflict of Interest statement.* None declared.

### REFERENCES

- Hagberg, B., Aicardi, J., Dias, K. and Ramos, O. (1983) A progressive syndrome of autism, dementia, ataxia, and loss of purposeful hand use in girls: Rett's syndrome: report of 35 cases. *Ann. Neurol.*, **14**, 471–479.
- Hagberg, B. (1985) Rett's syndrome: prevalence and impact on progressive severe mental retardation in girls. *Acta Paediatr. Scand.*, **74**, 405–408.
- Hagberg, B. (2002) Clinical manifestations and stages of Rett Syndrome. *Ment. Retard. Dev. Disabil. Res. Rev.*, **8**, 61–65.
- Amir, R.E. (1999) Rett syndrome is caused by mutations in X-linked MECP2, encoding methyl-CpG-binding protein 2. *Nat. Genet.*, **23**, 185–188.
- Wan, M., Lee, S.S., Zhang, X., Houwink-Manville, I., Song, H.R., Amir, R.E., Budden, S., Naidu, S., Pereira, J.L., Lo, I.F. *et al.* (1999) Rett syndrome and beyond: recurrent spontaneous and familial MECP2 mutations at CpG hotspots. *Am. J. Hum. Genet.*, **65**, 1520–1529.
- Renieri, A., Meloni, I., Longo, I., Ariani, F., Mari, F., Pescucci, C. and Cambi, F. (2003) Rett syndrome: the complex nature of a monogenic disease. *J. Mol. Med.*, **81**, 346–354.
- Zappella, M., Meloni, I., Longo, I., Hayek, G. and Renieri, A. (2001) Preserved speech variants of the Rett syndrome: molecular and clinical analysis. *Am. J. Med. Genet.*, **104**, 14–22.
- Zappella, M., Meloni, I., Longo, I., Canitano, R., Hayek, G., Rosaia, L., Mari, F. and Renieri, A. (2003) Study of MECP2 gene in Rett syndrome variants and autistic girls. *Am. J. Med. Genet. B Neuropsychiatr. Genet.*, **119**, 102–107.
- Shahbazian, M.D. and Zoghbi, H.Y. (2002) Rett syndrome and MeCP2: linking epigenetics and neuronal function. *Am. J. Hum. Genet.*, **71**, 1259–1272.
- Scala, E., Ariani, F., Mari, F., Caselli, R., Pescucci, C., Longo, I., Meloni, I., Giachino, D., Bruttini, M., Hayek, G. *et al.* (2005) CDKL5/STK9 is mutated in Rett syndrome variant with infantile spasms. *J. Med. Genet.*, **42**, 103–107.
- Tao, J., Van Esch, H., Hagedorn-Greife, M., Hoffmann, K., Moser, B., Raynaud, M., Sperner, J., Fryns, J.P., Schwinger, E., Gécz, J. *et al.* (2004) Mutations in the X-linked cyclin-dependent kinase-like 5 (CDKL5/STK9) gene are associated with severe neurodevelopmental retardation. *Am. J. Hum. Genet.*, **75**, 1149–1154.
- Weaving, L.S., Christodoulou, J., Williamson, S.L., Friend, K.L., McKenzie, O.L.D., Archer, H., Evans, J., Clarke, A., Pelka, G.J., Tam, P.P.L. *et al.* (2004) Mutations of CDKL5 cause a severe neurodevelopmental disorder with infantile spasms and mental retardation. *Am. J. Hum. Genet.*, **75**, 1079–1093.
- Nan, X., Campoy, F.J. and Bird, A. (1997) MeCP2 is a transcriptional repressor with abundant binding sites in genomic chromatin. *Cell*, **88**, 471–481.
- Jones, P.L., Veenstra, G.J., Wade, P.A., Vermaak, D., Kass, S.U., Landsberger, N., Strouboulis, J. and Wolffe, A.P. (1998) Methylated DNA and MeCP2 recruit histone deacetylase to repress transcription. *Nat. Genet.*, **19**, 187–191.
- Nan, X., Ng, H.H., Johnson, C.A., Laherty, C.D., Turner, B.M., Eisenman, R.N. and Bird, A. (1998) Transcriptional repression by the methyl-CpG-binding protein MeCP2 involves a histone deacetylase complex. *Nature*, **393**, 386–389.
- Kaludov, N.K. and Wolffe, A.P. (2000) MeCP2 driven transcriptional repression *in vitro*: selectivity for methylated DNA, action at a distance and contacts with the basal transcriptional machinery. *Nucleic Acids Res.*, **28**, 1921–1928.
- Georgel, P.T., Horowitz-Scherer, R.A., Adkins, N., Woodcock, C.L., Wade, P.A. and Hansen, J.C. (2003) Chromatin compaction by human MeCP2. Assembly of novel secondary chromatin structures in the absence of DNA methylation. *J. Biol. Chem.*, **278**, 32181–32188.
- Guy, J., Hendrich, B., Holmes, M., Martin, J.E. and Bird, A. (2001) A mouse MeCP2-null mutation causes neurological symptoms that mimic Rett syndrome. *Nat. Genet.*, **27**, 322–326.

19. Chen, R.Z., Akbarian, S., Tudor, M. and Jaenisch, R. (2001) Deficiency of methyl-CpG binding protein-2 in CNS neurons results in a Rett-like phenotype in mice. *Nat. Genet.*, **27**, 327–331.
20. Luikenhuis, S., Giacometti, E., Beard, C.F. and Jaenisch, R. (2004) Expression of MeCP2 in postmitotic neurons rescues Rett syndrome in mice. *Proc. Natl Acad. Sci. USA*, **101**, 6033–6038.
21. Mullaney, B.C., Johnston, M.V. and Blue, M.E. (2004) Developmental expression of methyl-CpG binding protein 2 is dynamically regulated in the rodent brain. *Neuroscience*, **123**, 939–949.
22. Ng, H.H. and Bird, A. (1999) DNA methylation and chromatin modification. *Curr. Opin. Genet. Dev.*, **9**, 158–163.
23. Tudor, M., Akbarian, S., Chen, R.Z. and Jaenisch, R. (2002) Transcriptional profiling of a mouse model for Rett syndrome reveals subtle transcriptional changes in the brain. *Proc. Natl Acad. Sci. USA*, **99**, 15536–15541.
24. Traynor, J., Agarwal, P., Lazzaroni, L. and Francke, U. (2002) Gene expression patterns vary in clonal cell cultures from Rett syndrome females with eight different MECP2 mutations. *BMC Med. Genet.*, **3**, 12.
25. Stancheva, I., Collins, A.L., Van den Veyver, I.B., Zoghbi, H. and Meehan, R.R. (2003) A mutant form of MeCP2 protein associated with human Rett syndrome cannot be displaced from methylated DNA by notch in *Xenopus* embryos. *Mol. Cell.*, **12**, 425–435.
26. Chen, W.G., Chang, Q., Lin, Y., Meissner, A., West, A.E., Griffith, E.C., Jaenisch, R. and Greenberg, M.E. (2003) Derepression of BDNF transcription involves calcium-dependent phosphorylation of MeCP2. *Science*, **302**, 885–889.
27. Martinowich, K., Hattori, D., Wu, H., Fouse, S., He, F., Hu, Y., Fan, G. and Sun, Y.E. (2003) DNA methylation-related chromatin remodeling in activity-dependent BDNF gene regulation. *Science*, **302**, 890–893.
28. Montini, E., Andolfi, G., Caruso, A., Buchner, G., Walpole, S.M., Mariani, M., Consalez, G., Trump, D., Ballabio, A. and Franco, B. (1998) Identification and characterization of a novel serine–threonine kinase gene from the Xp22 region. *Genomics*, **51**, 427–433.
29. Shahbazian, M.D., Antalffy, B., Armstrong, D.L. and Zoghbi, H.Y. (2002) Insight into Rett syndrome: MeCP2 levels display tissue- and cell-specific differences and correlate with neuronal maturation. *Hum. Mol. Genet.*, **11**, 115–124.
30. Vacca, M., Filippini, F., Budillon, A., Rossi, V., Mercadante, G., Manzati, E., Gualandi, F., Bigoni, S., Trabanelli, C., Pini, G. *et al.* (2001) Mutation analysis of the MECP2 gene in British and Italian Rett syndrome females. *J. Mol. Med.*, **78**, 648–655.
31. Di Cunto, F., Calautti, E., Hsiao, J., Ong, L., Topley, G., Turco, E. and Dotto, G.P. (1998) Citron rho-interacting kinase, a novel tissue-specific ser/thr kinase encompassing the Rho–Rac-binding protein Citron. *J. Biol. Chem.*, **273**, 29706–29711.
32. Hagberg, B.A. and Skjeldal, O.H. (1994) Rett variants: a suggested model for inclusion criteria. *Pediatr. Neurol.*, **11**, 5–11.
33. Kalscheuer, V.M., Tao, J., Donnelly, A., Hollway, G., Schwinger, E., Kubart, S., Menzel, C., Hoeltzenbein, M., Tommerup, N., Eyre, H. *et al.* (2003) Disruption of the serine/threonine kinase 9 gene causes severe X-linked infantile spasms and mental retardation. *Am. J. Hum. Genet.*, **72**, 1401–1411.
34. Huopaniemi, L., Tyynismaa, H., Rantala, A., Rosenberg, T. and Alitalo, T. (2000) Characterization of two unusual RS1 gene deletions segregating in Danish retinoblastoma families. *Hum. Mutat.*, **16**, 307–314.
35. Ariani, F., Mari, F., Pescucci, C., Longo, I., Bruttini, M., Meloni, I., Hayek, G., Rocchi, R., Zappella, M. and Renieri, A. (2004) Real-time quantitative PCR as a routine method for screening large rearrangements in Rett syndrome: report of one case of MECP2 deletion and one case of MECP2 duplication. *Hum. Mutat.*, **24**, 172–177.
36. Livak K. 1997. Comparative Ct method. User Bulletin no. 2.
37. Suzuki, M., Yamada, T., Kihara-Negishi, F., Sakurai, T. and Oikawa, T. (2003) Direct association between PU.1 and MeCP2 that recruits mSin3A-HDAC complex for PU.1-mediated transcriptional repression. *Oncogene*, **22**, 8688–8698.
38. Schaeren-Wiemers, N. and Gerfin-Moser, A. (1993) A single protocol to detect transcripts of various types and expression levels in neural tissue and cultured cells: *in situ* hybridization using digoxigenin-labelled cRNA probes. *Histochemistry*, **100**, 431–440.